



Cite this: *Chem. Commun.*, 2021, 57, 3375

Received 30th November 2020,
Accepted 23rd February 2021

DOI: 10.1039/d0cc07801h

rsc.li/chemcomm

The molecular design of photo-curable and high-strength benzoxazine for 3D printing†

Yong Lu,^{‡a} Kok Wei Joseph Ng,^{‡b} Hui Chen,^a Xuelong Chen,^b
Song Kiat Jacob Lim,^a Weili Yan^b and Xiao Hu^{‡*abc}

Low viscosity photo-curable benzoxazines (BZs) are designed and synthesized for use in stereolithography 3D printing. An initial investigation shows that the thermally polymerized polybenzoxazines (PBZs) have remarkably high T_g (264 °C) and flexural modulus (4.91 GPa) values. Subsequently, the formulated photoprintable resins are employed for use in high-resolution projection micro-stereolithography (PμSL) printing. Complex PBZ 3D structures can be achieved from the as-printed objects after they are thermally treated. These findings advance the design of BZ monomers for photopolymerization-based 3D printing and offer a method for the efficient fabrication of high-performance thermosets for various demanding engineering applications.

Polybenzoxazines (PBZs) are a class of high-performance thermosetting phenolics which have demonstrated a range of desirable features to overcome some drawbacks of using conventional novolac and resole type phenolics.^{1–3} Normally, they have high thermal stability and mechanical strength, high char yield, excellent flame resistance, low water absorption and near-zero volumetric shrinkage.^{4–7} Therefore, a variety of applications have been explored for using PBZs in important fields such as corrosion protection coatings, electronics, aerospace composites, blends and alloys.^{8–13} Although PBZs offer a variety of advantages, there are some inherent shortcomings that they face, such as their brittle natures and undesirable processability due to the high curing temperatures (generally 180–250 °C) required. Therefore, use of conventional manufacturing methods such as extrusion and melting are difficult to process PBZs into complicated structures and this limits their wide implementation.^{14–16}

Additive manufacturing (AM), commonly known as 3D printing, is a rapidly developing technology that has advanced product fabrication in prototyping and tooling, and has provided a revolutionary alternative for material processing away from traditional manufacturing methods, with the major advantage of accurately producing complex structures/shapes.^{17,18} Amongst various AM technologies, photopolymerization-based 3D printing using technologies such as stereolithography (SLA), digital light processing (DLP), and continuous liquid interface production (CLIP) have attracted special attention from material scientists and engineers due to the feasibility of obtaining high resolution and low feature sized products.¹⁹ A large number of polymer materials which are difficult to process and manipulate with traditional manufacturing methods have been successfully fabricated, normally *via* two-stage processing, into complex structures by photopolymerization-based 3D printing.^{20–22} Two new low viscosity photo-curable BZs, BZ-C2 and BZ-C5, for high-resolution PμSL processing are reported here. Studies of the corresponding PBZs show excellent thermal and mechanical properties, indicating their high-performance characteristics. The PBZ 3D structured objects are demonstrated, which are produced by thermally curing the PμSL printed parts. These findings establish the BZ monomer design for favourable photo resins, offer a way for PBZ fabrication using high-resolution PμSL printing, and also benefit the approach of processing high-performance thermosets with AM technology for demanding functional applications.

The synthetic approach to the monoacrylate functionalized BZ-C2 and BZ-C5, as well as a diacrylate functionalized BZ-BA is shown in Fig. 1a. A typical Mannich condensation was used first, to synthesize the hydroxyl-terminated BZs. Phenol/bisphenol A (BPA), 2-aminoethanol/5-amino-1-pentanol and paraformaldehyde were reacted in chloroform (CHCl₃) solution at 70 °C overnight. Afterwards, the reaction mixture was washed with an alkaline solution to remove unreacted acidic impurities, followed by a generalized aqueous workup to yield the desired products. The as-prepared hydroxyl BZs were continuously reacted with acryloyl chloride to form the acrylate functionalized BZs and their chemical structures were verified by ¹H-NMR and

^a Temasek Laboratories@NTU, Nanyang Technological University, Research Techno Plaza, 50 Nanyang Drive, 637553, Singapore

^b School of Materials Science and Engineering, Nanyang Technological University, 639798, Singapore. E-mail: ASXHU@ntu.edu.sg

^c Nanyang Environment and Water Research Institute, Nanyang Technological University, 637141, Singapore

† Electronic supplementary information (ESI) available. See DOI: 10.1039/d0cc07801h

‡ These authors contributed equally.

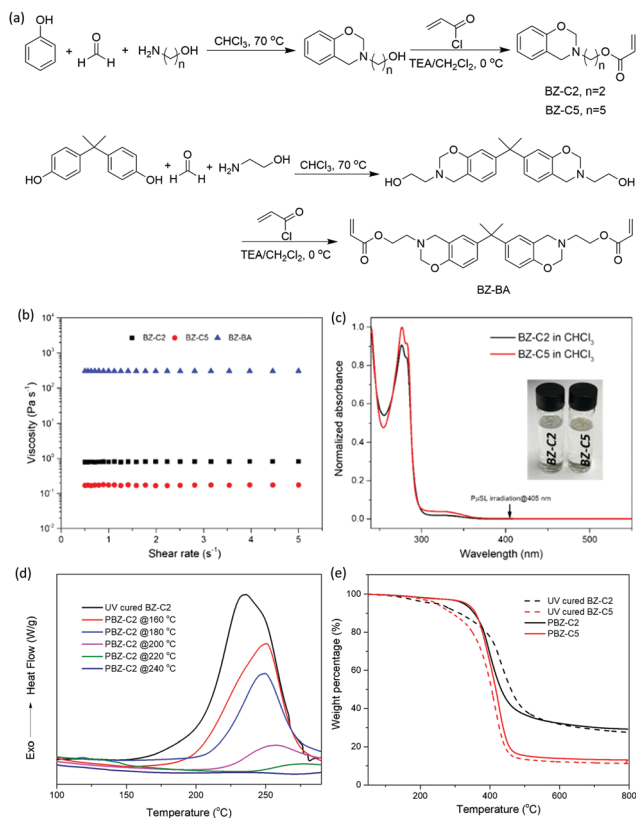


Fig. 1 (a) Synthetic routes, and (b) plots of viscosity vs. shear rate for BZ-C2, BZ-C5, and BZ-BA. (c) UV-vis absorption spectra of BZ-C2 and BZ-C5 in dilute chloroform solution. (d) DSC thermograms for PBZ-C2 cured at different temperatures. (e) The TGA curves of photocured BZ-C2/C5 and PBZ-C2/C5 under a N₂ atmosphere.

FT-IR resonances. As shown in Fig. S1a and b (ESI[†]), the characteristic proton resonances (Ar-CH₂-N- and -O-CH₂-N-) of the oxazine ring appear at 4.85 and 4.05 ppm for BZ-C2 and at 4.83 and 3.96 ppm for BZ-C5. The multiplets in the range of 7.13 – 6.77 ppm and 7.09 – 6.75 ppm are assigned to their aromatic protons. The peaks at 6.42, 6.14, 5.85 ppm in Fig. S1a (ESI[†]) are assigned to the vinyl protons of BZ-C2. In Fig. S1b (ESI[†]), the chemical shifts at 6.38, 6.10, 5.79 ppm belonged to the vinyl protons of BZ-C5. The structure of BZ-BA is verified with ¹H-NMR as well (Fig. S1c, ESI[†]). The FT-IR absorption results further confirm the chemical structures of BZ-C2 and BZ-C5. As can be seen from Fig. S2a (ESI[†]), the characteristic absorption band of C–O–C and N–C–O of the oxazine ring are clearly observed at ~1224 and ~935 cm⁻¹, respectively. Meanwhile, the stretching absorption of the carbonyl and vinyl groups in the acrylate structure are found at about 1718 and 1638 cm⁻¹, respectively. These results prove the successful synthesis of the acrylate BZs.

The viscosity data of the BZ monomers were collected using a rotational rheometer with parallel plate geometry at ambient temperature. The shear rate was varied in the range from 0.5 to 5 s⁻¹. Fig. 1b shows that the viscosity of BZ-BA, BZ-C2 and BZ-C5 is 300, 0.9 and 0.1 Pa s⁻¹, respectively. Obviously, the diacrylate BZ-BA monomer has a much higher viscosity than the monoacrylate-based BZ-C2 and BZ-C5 due to its comparatively

large molecule structure. It has been reported that the viscosity of a photopolymerization printable formulation should be in the order of 5 Pa s⁻¹, otherwise, the printing resin is not able to flow sufficiently and recover the building platform evenly if the viscosity is higher than this value.²³ Due to the highly viscous nature, BZ-BA is not suitable for formulating a photo-curable resin without adequate addition of monomer diluents. Moreover, BZ-BA has poor stability in air and can gelatinize within several hours. Conversely, BZ-C2 and BZ-C5 are fairly stable and possess a low viscosity, which is favourable for photo-curable resins. In Fig. 1c, the UV-vis absorption of BZ-C2 and BZ-C5 in dilute CHCl₃ is shown and both of them exhibit similar absorption bands with a maximum absorption at 277 nm. Because they do not show UV-vis absorption beyond 400 nm, the resins based on them will not affect the light penetration of the UV light source with a wavelength longer than 400 nm.

In order to obtain PBZ structures of the two BZ monomers, thermal polymerization of BZ-C2 was examined using DSC analysis. The sample was prepared with a dual-curing process, in which the BZ-C2 monomer and the photo initiator BAPO were mixed vigorously with a vortex mixer to form a homogeneous resin. The resin was deposited in a silicone mould and solidified within ~10 s under UV irradiation. The photo curing process was continued until full cure of the samples occurred, as shown by the significantly decreased FT-IR absorption of the vinyl structure (Fig. S2, ESI[†]). Afterwards, a progressive thermal treatment was applied to the photocured sample and a specimen was collected at each curing stage for DSC scanning. As presented in Fig. 1d, the photocured BZ-C2 exhibited a broad exothermic peak at 235 °C (onset at 162 °C), corresponding to the oxazine ring-opening polymerization. Being thermally treated from 160 to 220 °C, the exothermic peak decreases gradually at each stage, indicating the consecutive ring-opening of the BZs and the incomplete PBZ network within the sample. When the curing temperature reaches 240 °C, the exotherm disappears completely, suggesting that entire conversion to the PBZ network has occurred. Therefore, the maximum treatment temperature of 240 °C was applied to all thermal curing processes in this work. The thermal stability of the resultant PBZs was examined using TGA analysis in a N₂ atmosphere. Fig. 1e shows that the 5% and 10% weight loss temperatures (*T*₅ and *T*₁₀) of photocured BZ-C2 are 252 and 314 °C, which are significantly improved to 326 and 358 °C, respectively, for the resultant PBZ-C2. Similar findings are observed for photocured BZ-C5 as well, with the *T*₅ and *T*₁₀ enhanced from 249 and 292 °C to 327 and 360 °C, respectively, after thermal curing. The greatly increased thermal stability of the PBZs is attributed to the highly crosslinked network in their structures. Interestingly, both PBZ-C2 and PBZ-C5 exhibit a similar initial degradation temperature because the network degradation is always initiated from the cleavage of their Mannich base formed by ring-opening. After the initial degradation, all the tested samples display a second thermal degradation attributed to the thermal decomposition of the polymer main chains. It is worth noting that the char yield at 800 °C for PBZ-C2 is ~30%, which is much higher than that of the commercial resin (~7%) (Fig. S3, ESI[†]), suggesting the

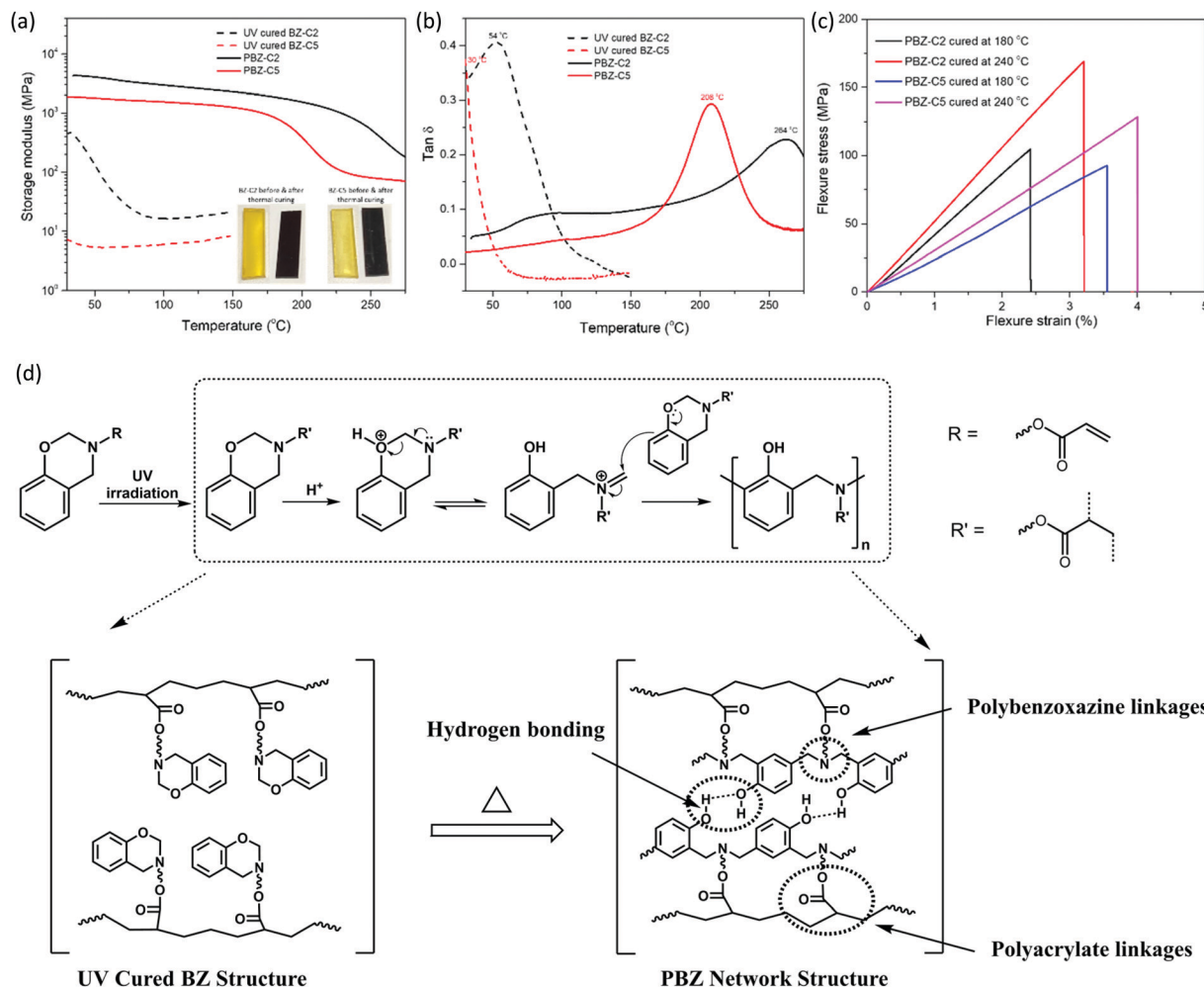


Fig. 2 (a) Storage moduli (insets: Specimen bars used for testing) and (b) $\tan \delta$ values plotted as functions of temperature for photocured BZ-C2/C5 and PBZ-C2/C5. (c) Flexure stress–strain curves of PBZ-C2 and PBZ-C5 thermally cured at different temperatures. (d) A general ring opening reaction mechanism and the corresponding network structures of UV cured BZ and PBZ.

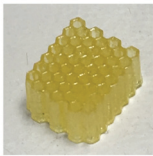


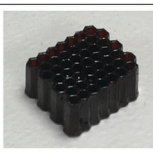


potential applications of flame retardants and carbon precursors for PBZ-C2.

The thermomechanical behaviours of photocured BZ-C2/C5 and PBZ-C2/C5 were studied using DMA. Fig. 2a and b show the temperature dependence of the storage modulus and $\tan \delta$, whereas the maximum value of the $\tan \delta$ curve is used to determine the T_g . For the photocured BZ-C2 and BZ-C5, the initial storage moduli are 478 and 7 MPa, respectively, and these decrease sharply as the temperature rises, indicating the elastomer behaviour of the samples. However, PBZ-C2 and PBZ-C5 exhibit remarkably enhanced initial storage moduli of 4.3 and 1.9 GPa, respectively, which are maintained at temperatures up to nearly 150 °C. Additionally, a T_g of 54 °C and less than 30 °C is found for the photocured BZ-C2 and BZ-C5, respectively, whereas PBZ-C2 and PBZ-C5 showed highly improved T_g of 264 and 208 °C, respectively. Considering the dual curing process of photo and thermal photopolymerization as well as the intermolecular hydrogen bonding formed (Fig. 2d), a triple network (Fig. S4, ESI[†]) is eventually established within the PBZ structures and this contributes mostly to

the significantly enhanced storage modulus and T_g . In particular, the broad $\tan \delta$ peaks of the PBZ-C2 and PBZ-C5 curves suggest that there is a heterogenous network in their structures, consisting of both highly and loosely crosslinked regions. Encouraged by the DMA results, the mechanical performances of PBZ-C2 and PBZ-C5 were further studied with a 3-point bending test and representative flexure stress–strain curves are shown in Fig. 2c. As shown, the modulus of the PBZs is greatly improved with the progressive thermal treatment due to the increased crosslinking of the samples. Remarkable moduli of 4.91 and 3.00 GPa are achieved for the fully cured PBZ-C2 and PBZ-C5, respectively. As shown in Fig. S5 (ESI[†]), compared to commonly used plastic resins, both PBZ-C2 and PBZ-C5 demonstrate high T_g and moduli which are associated with photo printability, indicating that the two PBZs are high-performance thermosets with excellent and promising properties.

Due to their low viscosity and interesting features of the resultant PBZs, BZ-C2 and BZ-C5 monomers were formulated into photo resins to demonstrate their use in manufacturing

Table 1 The diverse 3D printed structures and height changes before and after thermal treatment

3D Printed structures	Honeycomb ^a	Gear ^b	Component ^b
As-printed (height, mm)	 3.10 ± 0.04	 4.35 ± 0.03	 5.18 ± 0.03
Thermally cured@240 °C (height, mm)*	 3.06 ± 0.03 (-1.3 %)	 4.23 ± 0.04 (-2.3 %)	 5.08 ± 0.02 (-2.0 %)

*Height change percentage in brackets. ^a BZ-C5 based resin. ^b BZ-C2 based resin.

high-performance PBZ thermosets with a two-stage fabrication process, consisting of PμSL 3D printing and post thermal curing. For the PμSL printing, a UV light source with a wavelength of 405 nm and an intensity of 17.5 mW cm⁻² were used for all the printing. The formulated resin was exposed to UV irradiation for 6 s per layer and generated a designed pattern with roughly 100 μm thicknesses. As the printing process progressed, the structural geometry was built up in a layer-by-layer manner. Once the printing was completed, the structure was removed, photocured further and transferred for a second stage thermal curing. Table 1 demonstrates the printed objects with various 3D structures before and after thermal treatment. Measured using a micrometre calliper, only small height shrinkages are detected for the resultant PBZ structures. As shown from the SEM scans in Fig. S6 (ESI[†]), there are no bubbles or voids on the PBZ fracture surfaces, suggesting a smooth post cure without release of volatile compounds. The results show that the formulation based on BZ-C2 and BZ-C5 monomers is suitable for PμSL 3D printing, and consequently, high-performance PBZ structured objects can be achieved.

In summary, two monoacrylate-functionalized BZs, BZ-C2 and BZ-C5, which have photo- and thermal-curing mechanism, were synthesized and characterized. Their chemical structures are verified *via* ¹H-NMR and FT-IR spectra to confirm the successful synthesis. Both BZ monomers exhibit fairly low viscosity and desirable UV absorption, which are favourable for formulating a photopolymerization resin. The DSC studies show that PBZ structures can be readily achieved from photocured BZ-C2 and BZ-C5 *via* scheduled thermal treatment. The resulting PBZ-C2 and PBZ-C5 exhibit greatly improved thermal stability, highly enhanced *T_g* values, and excellent mechanical performances. In particular, PBZ-C2 exhibits a *T_g* value as high

as 264 °C and a remarkable flexural modulus of 4.91 GPa due to the highly crosslinked triple network within its structure. PBZ objects with complex 3D structures are demonstrated using PμSL printing and follow-up post-curing. The benefits of this work are that it expands the existing library with a new class of PBZs for popular additive manufacturing and it explores an approach for processing high-performance thermosets for various advanced applications.

The authors acknowledge support from the Nanyang Technological University (NTU) with grant number: 04IDS000677N040 and support from the School of Materials Science and Engineering NTU for the present work. The authors also acknowledge Lim Zhi Han Chester for his help with designing and generating the CAD files.

Nanyang Technological University, Singapore, is filing a patent based on this work.

Conflicts of interest

There are no conflicts to declare.

References

- 1 C. P. R. Nair, *Prog. Polym. Sci.*, 2004, **29**, 401–498.
- 2 N. N. Ghosh, B. Kiskan and Y. Yagci, *Prog. Polym. Sci.*, 2007, **32**, 1344–1391.
- 3 S. Wirasate, S. Dhumrongvaraporn, D. J. Allen and H. Ishida, *J. Appl. Polym. Sci.*, 1998, **70**, 1299–1306.
- 4 Y. Yagci, B. Kiskan and N. N. J. Ghosh, *J. Polym. Sci., Part A: Polym. Chem.*, 2009, **47**, 5565–5576.
- 5 Y. X. Wang and H. Ishida, *J. Appl. Polym. Sci.*, 2002, **86**, 2953–2966.
- 6 H. D. Kim and H. Ishida, *Macromolecules*, 2003, **36**, 8320–8329.
- 7 L. Dumas, L. Bonnaud, M. Olivier, M. Poorteman and P. Dubois, *Chem. Commun.*, 2013, **49**, 9543–9545.
- 8 B. Kiskan, *React. Funct. Polym.*, 2018, **129**, 76–88.
- 9 M. Monisha, N. Amarnath, S. Mukherjee and B. Lochab, *Macromol. Chem. Phys.*, 2019, **220**, 1800470.
- 10 L. Lin, H. Yen, C. Chen, C. Tsai and G. Liou, *Chem. Commun.*, 2014, **50**, 13917–13920.
- 11 S. Rimdusit, S. Tiptipakon, C. Jubsilp and T. Takeichi, *React. Funct. Polym.*, 2013, **73**, 369–380.
- 12 N. K. Sini, J. Bijwe and I. K. J. Varma, *J. Polym. Sci., Part A: Polym. Chem.*, 2014, **52**, 7–11.
- 13 H. Ishida and S. Ohba, *Polymer*, 2005, **46**, 5588–5595.
- 14 Y. Yagci, B. Kiskan and N. N. Ghosh, *J. Polym. Sci., Part A: Polym. Chem.*, 2009, **47**, 5565–5576.
- 15 B. Kiskan, B. Koz and Y. Yagci, *J. Polym. Sci., Part A: Polym. Chem.*, 2009, **47**, 6955–6961.
- 16 T. Agag, S. Geiger, S. M. Alhassan, S. Qutubuddin and H. Ishida, *Macromolecules*, 2010, **43**, 7122–7127.
- 17 B. Narupai and A. Nelson, *ACS Macro Lett.*, 2020, **9**, 627–638.
- 18 S. C. Ligon, R. Liska, J. Stampfl, M. Gurr and R. Mülhaupt, *Chem. Rev.*, 2017, **117**, 10212–10290.
- 19 J. Zhang and P. Xiao, *Polym. Chem.*, 2018, **9**, 1530–1540.
- 20 M. Hegde, V. Meenakshisundaram, N. Chartrain, S. Sekhar, D. Tafti, C. B. Williams and T. E. Long, *Adv. Mater.*, 2017, **29**, 1701240.
- 21 J. Herzberger, V. Meenakshisundaram, C. B. Williams and T. E. Long, *ACS Macro Lett.*, 2018, **7**, 493–497.
- 22 J. J. Weigand, C. I. Miller, A. P. Janisse, O. D. McNair, K. Kim and J. S. Wiggins, *Polymer*, 2020, **189**, 122193.
- 23 F. P. W. Melchels, J. Feijen and D. W. Grijpma, *Biomaterials*, 2010, **31**, 6121–6130.